

available at [www.sciencedirect.com](http://www.sciencedirect.com)journal homepage: [www.eu-openscience.europeanurology.com](http://www.eu-openscience.europeanurology.com)

European Association of Urology



## Bladder Cancer

# Human Gut Mycobiome and Fungal Community Interaction: The Unknown Musketeer in the Chemotherapy Response Status in Bladder Cancer

Laura Bukavina<sup>a,b,c,\*</sup>, Megan Prunty<sup>a</sup>, Ilaha Isali<sup>a,b</sup>, Adam Calaway<sup>a,b</sup>, Rashida Ginwala<sup>c</sup>, Mohit Sindhani<sup>d</sup>, Mahmoud Ghannoum<sup>b,e</sup>, Kirtishri Mishra<sup>a,b</sup>, Alexander Kutikov<sup>c</sup>, Robert G. Uzzo<sup>c</sup>, Lee E. Ponsky<sup>a,b</sup>, Philip H. Abbosh<sup>e,f</sup>

<sup>a</sup> Department of Urology, University Hospitals, Cleveland, OH, USA; <sup>b</sup> Case Comprehensive Cancer Center, Cleveland, OH, USA; <sup>c</sup> Fox Chase Cancer Center, Philadelphia, PA, USA; <sup>d</sup> India Institute of Technology, Delhi, India; <sup>e</sup> Department of Pathology and Dermatology, Case Western School of Medicine, Cleveland, OH, USA; <sup>f</sup> Albert Einstein Medical Center, Philadelphia, PA, USA

### Article info

#### Article history:

Accepted June 22, 2022

#### Associate Editor:

M. Carmen Mir

#### Keywords:

Mycobiome  
Bladder cancer  
Urothelial cancer  
Microbiome

### Abstract

**Background:** Until recently, the properties of microbiome and mycobiome in humans and its relevance to disease have largely been unexplored. While the interest of microbiome and malignancy over the past few years have burgeoned with advent of new technologies, no research describing the composition of mycobiome in bladder cancer has been done. Deciphering of the metagenome and its aggregate genetic information can be used to understand the functional properties and relationships between the bacteria, fungi, and cancer.

**Objective:** The aim of this project is to characterize the compositional range of the normal versus bladder cancer mycobiome of the gut.

**Design, setting, and participants:** An internal transcribed spacer (ITS) survey of 52 fecal samples was performed to evaluate the gut mycobiome differences between noncancer controls and bladder cancer patients.

**Outcome measurements and statistical analysis:** Our study evaluated the differences in mycobiome among patients with bladder cancer, versus matched controls. Our secondary analysis evaluated compositional differences in the gut as a function of response status with neoadjuvant chemotherapy. Data demultiplexing and classification were performed using the QIIME v.1.1.1.1 platform. The Ion Torrent-generated fungal ITS sequence data were processed using QIIME (v.1.9.1), and the reads were demultiplexed, quality filtered, and clustered into operation taxonomic units using default parameters. Alpha and beta diversity were computed and plotted in Phyloseq, principal coordinate analysis was performed on Bray-Curtis dissimilarity indices, and a one-way permutational multivariate analysis of variance was used to test for significant differences between cohorts. Phylogenetic Investigation of Communities by Reconstruction of Unobserved States (PICRUST)

\* Corresponding author. Division of Urologic Oncology, Fox Chase Cancer Center, Temple University School of Medicine, 333 Cottmann Ave, Philadelphia, PA 19111, USA. Tel. +1 2162624392. E-mail address: [Laura.Bukavina@fcc.edu](mailto:Laura.Bukavina@fcc.edu) (L. Bukavina).

<https://doi.org/10.1016/j.euros.2022.06.005>

2666-1683/© 2022 The Authors. Published by Elsevier B.V. on behalf of European Association of Urology. This is an open access article under the CC BY-NC-ND license (<http://creativecommons.org/licenses/by-nc-nd/4.0/>).



was applied to infer functional categories associated with taxonomic composition. **Results and limitations:** We found distinctive mycobiome differences between control group ( $n = 32$ ) and bladder cancer ( $n = 29$ ) gut flora, and identified an increasing abundance of *Tremellales*, *Hypocreales*, and *Dothideales*. Significant differences in alpha and beta diversity were present between the groups (control vs bladder;  $p = 0.002$ ), noting distinct compositions within each cohort. A subgroup analysis by sex and neoadjuvant chemotherapy status did not show any further differences in mycobiome composition and diversity. Our results indicate that the gut mycobiome may modulate tumor response to preoperative chemotherapy in bladder cancer patients. We propose that patients with a “favorable” mycobiome composition (eg, high diversity, and low abundance of *Agaricomycetes* and *Saccharomycetes*) may have enhanced systemic immune response to chemotherapy through antigen presentation.

**Conclusions:** Our study is the first to characterize the enteric mycobiome in patients with bladder cancer and describe complex ecological network alterations, indicating complex bacteria-fungi interactions, particularly highlighted among patients with complete neoadjuvant chemotherapy response.

**Patient summary:** Our study has demonstrated that the composition of stool mycobiome (fungal inhabitants of the gastrointestinal tract) in patients with bladder cancer is different from that in noncancer individuals. Furthermore, when evaluating how patients respond to chemotherapy given prior to their surgery, our study noted significant differences between patients who responded and those who did not.

© 2022 The Authors. Published by Elsevier B.V. on behalf of European Association of Urology. This is an open access article under the CC BY-NC-ND license (<http://creativecommons.org/licenses/by-nc-nd/4.0/>).

## 1. Introduction

Based on the American Cancer Society, estimated new diagnoses of bladder cancer (BCa) are 83 730 (64 280 in men and 19 450 in women) in 2021, accounting for 7% of all cancer cases and 5% of all cancer-related deaths [1,2]. Unfortunately, the etiology and pathogenesis of BCa are still not defined fully, and clinical management remains challenging.

A growing body of evidence has linked specific signatures of microbial clades to disease pathogenesis [3]. Although the bacteriome makes up the vast majority (>99%) of gut flora, commensal fungi or the “mycobiome” coexists and interacts in ways that affect the host organism [4]. Current scientific evidence supports the gut mycobiome’s contribution to host immune response, with clinical relevance to regional and systemic disease.

Fungal mycobiome is an understudied constituent in the pathogenesis of BCa. Herein, we characterize the differences in the gut mycobiome between healthy and BCa cohorts, evaluate the distribution of functional contents encoded by the predominant genera of the gut mycobiome, and assess the coevolved relationship between gut bacteria and fungi as a first step in identifying potentially tractable taxa. Furthermore, to better understand the role of mycobiome in response to neoadjuvant chemotherapy, we prospectively collected mycobiome samples from patients undergoing neoadjuvant chemotherapy prior to extirpative surgery. We tested the tumor response to preoperative chemotherapy, based on mycobiome composition of the gut, to define a favorable gut mycobiome with enhanced neoadjuvant chemotherapy response.

## 2. Patients and methods

### 2.1. Study design and patients

Human fecal samples were collected in compliance with the policies and approval of University Hospitals Cleveland Medical Center’s Institutional Review Board. We prospectively collected fecal samples, at least 2 cm from the anal verge, at the time of cystectomy before initiation of antibiotic prophylaxis. We excluded patients diagnosed with inflammatory bowel disease, those with a *Clostridium difficile* infection history, or those who had any antibiotic therapy in the last 6 wk. The following inclusion criteria were used: (1) age  $\geq 18$  and  $\leq 70$  yr, both male and female, and (2) undergoing cystectomy at our institution for biopsy-confirmed muscle-invasive BCa.

### 2.2. Collection of fecal samples

At the time of surgery, the urology provider collected a stool sample approximately 5–6 cm from the anus during the examination under anesthesia with digital rectal examination using sterile gloves. The stool was collected off the sterile glove with a sterile swab and placed into a 15-ml sterile cell culture conical tube containing 1 ml of phosphate-buffered saline (PBS). The swab was stored at 0°C during transport to the laboratory, within 2 h of collection. Samples were resuspended and stored in sterile PBS at  $-80^{\circ}\text{C}$  until analysis.

### 2.3. Extraction and sequencing of fungal DNA

Total genomic DNA was isolated and purified with the QIAamp DNA Mini Kit, as per the manufacturer’s instructions (Qiagen). The quality and purity of the isolated genomic DNA was confirmed spectrophotometrically using NanoDrop 2000 device (Thermo Fisher Scientific SAS, Illkirch, France). DNA concentration was quantified using the Qubit 2.0 instrument applying the Qubit dsDNA HS Assay (Life Technologies,

USA). Extracted DNA samples were stored at  $-20^{\circ}\text{C}$ . Briefly, the internal transcribed spacer (ITS; ITS2) regions of the rRNA cistron were amplified using ITS1 (5'-TCC GTA GGT GAA CCT GCG G-3') and ITS4 (5'-TCC TCC GCT TAT TGA TAT GC-3') primers [5]. Polymerase chain reactions (PCRs) were carried out on 100 ng template DNA, in 50  $\mu\text{l}$  (final volume) reaction mixture consisting of Dream Taq Green PCR Master Mix (Thermo Fisher Scientific), 0.1 g/l bovine serum albumin, 1% of dimethyl sulfoxide, 6 mM  $\text{MgCl}_2$ , and a final primer concentration of 400 nM. PCR conditions were initial denaturation at  $94^{\circ}\text{C}$  for 3 min, 35 cycles of denaturation for 30 s each at  $94^{\circ}\text{C}$ , annealing at  $50^{\circ}\text{C}$  for 30 s, extension at  $72^{\circ}\text{C}$  for 1 min, and final extension at  $72^{\circ}\text{C}$  for 5 min. Following the 35 cycles, there was a final extension time of 30 min to minimize artifacts induced by TAQ polymerase. Amplicon library was generated with PCR products using Ion plus Fragment Library kits (<350 bp) according to the manufacturer's instructions, and the library was barcoded with Ion Xpress Barcode Adapter and ligated with the A and P1 adaptors.

#### 2.4. Sequencing, classification, and analysis

The adapted barcoded libraries were equalized using the Ion Library Equalizer kit to a final concentration of 100 pM, pooled and diluted to 26 pM, and attached to the surface of Ion Sphere particles (ISPs) using an Ion Personal Genome Machine (PGM) Template OT2 200bp kit v2 (Life Technologies) according to the manufacturer's instructions, via emulsion PCR. Quality of ISPs templates was checked using Ion Sphere Quality Control Kit (part no. 4468656) with the Qubit 2.0 device. Sequencing of the pooled libraries was carried out on the Ion Torrent PGM system using the Ion Sequencing 200 kit v2 (all from Life Technologies) for 150 cycles (600 flows), with a 318-chip following the manufacturer's instructions. Demultiplexing and classification were performed using the QIIME v.1.1.1.1 platform [6]. The resulting sequence data were trimmed to remove adapters, barcodes, and primers during the demultiplexing process. In addition, bioinformatic process filters were applied to the sequence data for the removal of low-quality reads below Q25 Phred score and denoised to exclude sequences with read length below 100 bp. De novo operation taxonomic units (OTUs) were clustered using the Uclust algorithm and defined by 97% sequence similarity.

#### 2.5. Bioinformatics and statistical analyses

The Ion Torrent-generated fungal ITS sequence data were processed using QIIME (v.1.9.1), and the reads were demultiplexed, quality filtered, and clustered into OTUs using default parameters [7]. Chimeric sequences were removed using VSEARCH (v.2.4.3) with UNITE UCHIME reference dataset (v.7.2). OTUs were picked using the open reference OUT picking method, with default parameters, against the UNITE reference database (v.7.2) to assign taxonomy using `pick_open_reference_otus.py` [6]. For the analysis, only the amplicon sequence variants that matched the following criteria were included: a minimum read count of more than ten reads across all samples and taxonomies defined to at least order level. Alpha and beta diversity were computed and plotted in Phyloseq, principal coordinate analysis (PCoA) was performed on Bray-Curtis dissimilarity indices, and a one-way permutational multivariate analysis of variance was used to test for significant differences between cohorts (Adonis, R package Vegan v.2.4.5). The  $p$  values of  $<0.05$  were considered to be significant. Linear discriminant analysis (LDA) effect size (LEfSe) was used to identify significant differences in metagenomic taxa between healthy and BCa cohorts. The Shannon diversity index was used to quantify and compare mycobiome diversity across samples. A Phylogenetic Investigation of Communities by Reconstruction of Unobserved States (PICRUSt) analysis was performed to identify Kyoto Encyclopedia of Genes and Genomes (KEGG) metabolic pathways potentially represented by groups of fungi. The KEGG level 3

pathways were filtered for rare pathways by including only pathways with relative abundance  $>0.1\%$  in at least half of the samples, normalized to relative abundance, and tested for association with BCa /healthy and female/male conditions using nonparametric Wilcoxon rank-sum test followed by false discovery rate adjustment. PICRUSt is a bioinformatic software package designed to predict metagenome functional content from marker gene surveys and full genomes. PICRUSt was applied to infer functional categories associated with taxonomic composition. We utilized  $t$  tests for continuous variables and chi-square tests for categorical variables. Using the PICRUSt data, we compared continuous variables for metabolic function sets in healthy controls versus BCa patients.

#### 2.6. Response status analysis

Additionally, we evaluated compositional differences in the gut as a function of response status with neoadjuvant chemotherapy. Out of 29 patients, ten (34.4%) underwent neoadjuvant chemotherapy. In other words, complete response (CR;  $n = 3$ ), identified as pT0 disease at the time of cystectomy, versus no response (NR;  $n = 4$ ) with presence of disease within cystectomy specimen. Alpha diversity was estimated using the Inverse Simpson Index ( $D$ ), which captures the variance of taxonomic abundance as  $D = 1 / \sum_{k=1}^S p_i^2$ , where  $p_i$  is the proportion of the total species  $S$  that comprises the species  $i$  [8]. Limits were set based on the least number of reads in fecal samples (7000) that were analyzed. Results were also validated using other indices such as Chao1, Simpson, and Shannon [9,10]. The LEfSe method of analysis first compares abundances of all mycobiome clades (in this case between response and NR), using the Kruskal-Wallis test at a predefined  $\alpha$  of 0.05. Significantly different vectors resulting from the comparison of abundances between groups are used as input for LDA, which produces an effect size. The primary advantage of LEfSe over traditional statistical tests is that an effect size is produced. This allows sorting of results of multiple tests by the magnitude of the difference between groups.

### 3. Results

This study was performed with Institutional Review Board approval between September 2020 and May 2021, in patients with a diagnosis of muscle-invasive BCa undergoing cystectomy. Controls ( $n = 32$ ) were retrospectively collected from the biorepository of the Case Comprehensive Cancer Center, Cleveland, OH, matched for age, body mass index (BMI), and gender. To minimize confounding of known factors that effect mycobiome, we matched our BCa samples to our healthy cohort based on gender, age, and BMI. All samples were collected using the aseptic method and frozen to  $-20^{\circ}\text{C}$ . Within the cohort, there were 17 (58.6%) males and 12 (41.4%) females (Supplementary Table 1). The median (interquartile range) age and BMI were 74 y (63–77) and 28.7  $\text{kg}/\text{m}^2$  (25.9–32.1), respectively. There were no significant differences between the BCa and healthy cohorts aside from the history of BCa and smoking status. No patients underwent bowel preparation prior to collection of stool samples.

#### 3.1. Fungal diversity and composition in BCa patients versus healthy controls

*Saccharomycetales* dominated the fungal mycobiota community composition at order level with the mean relative abundance of 48.99% and 95.27% between BCa patients and healthy controls, respectively. *Hypocreales* was the

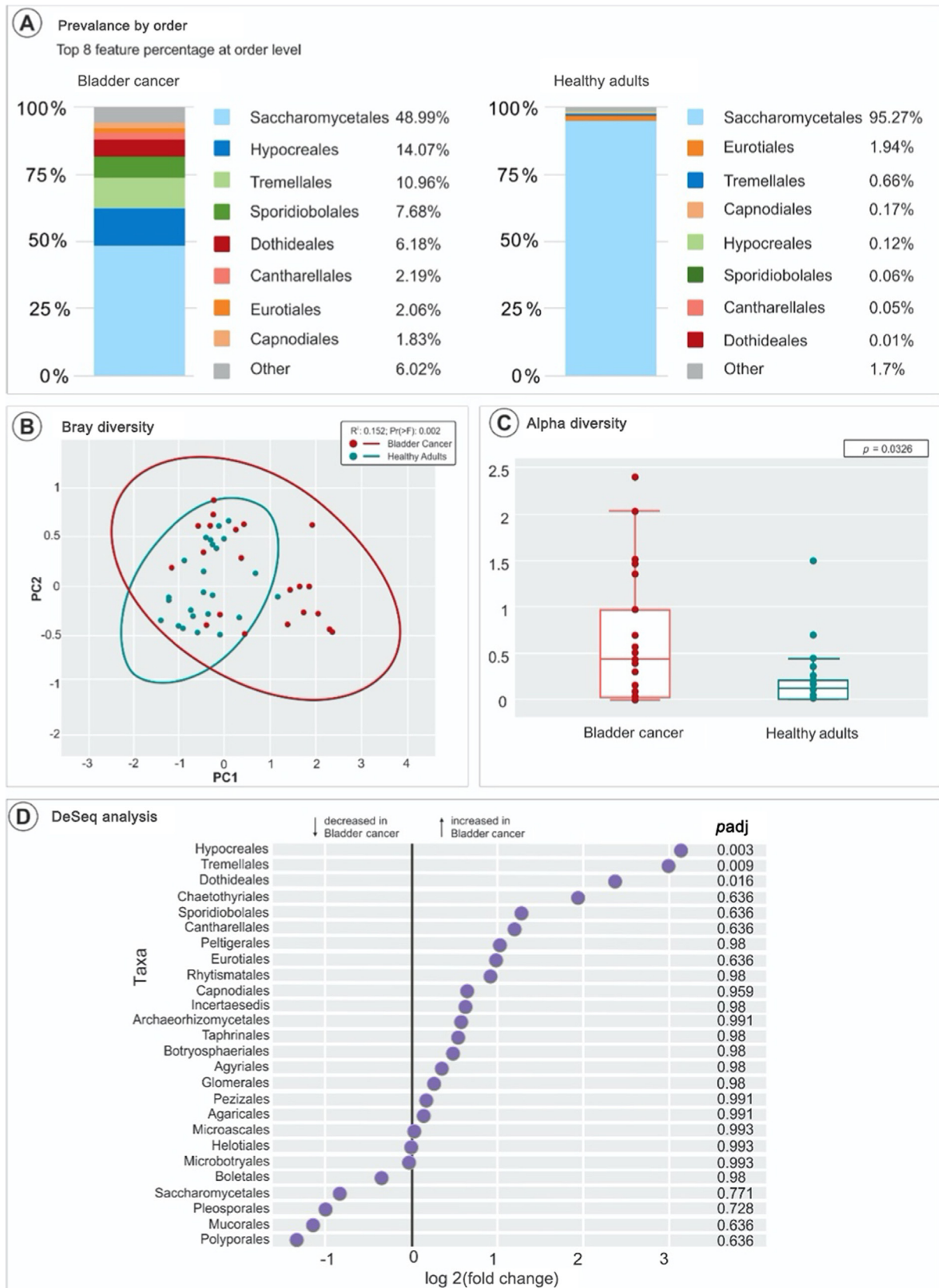
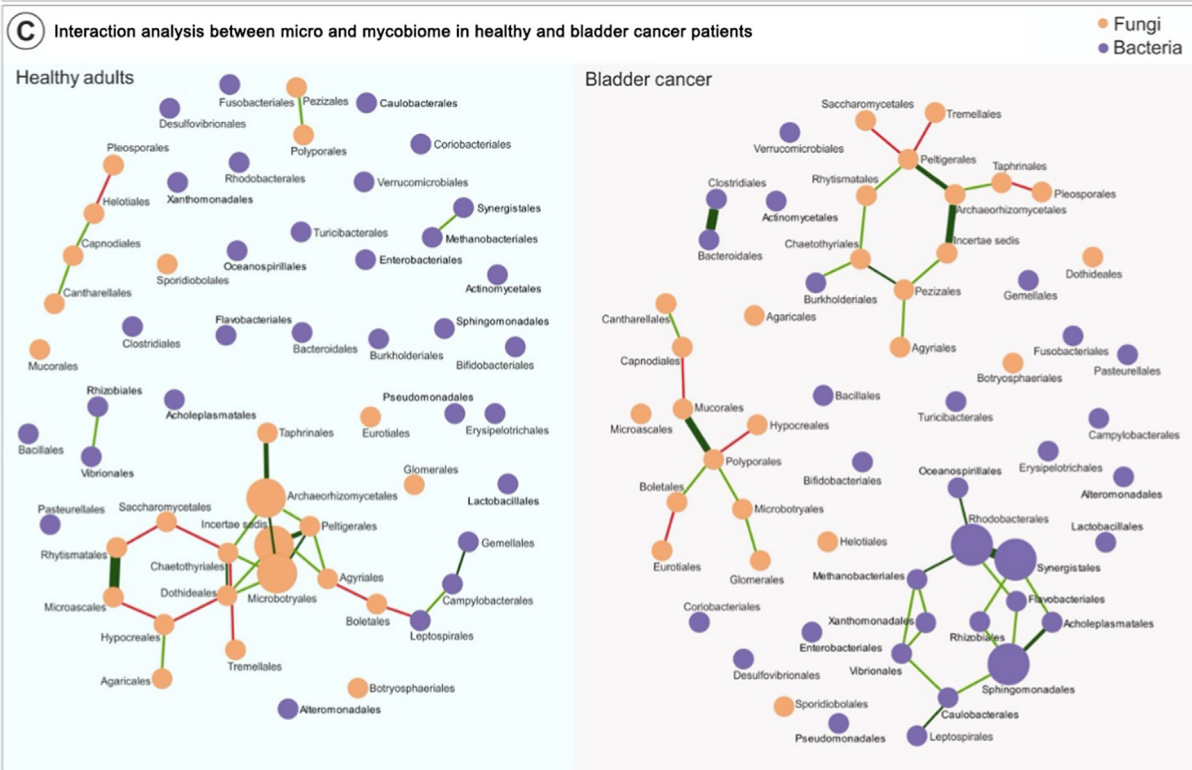
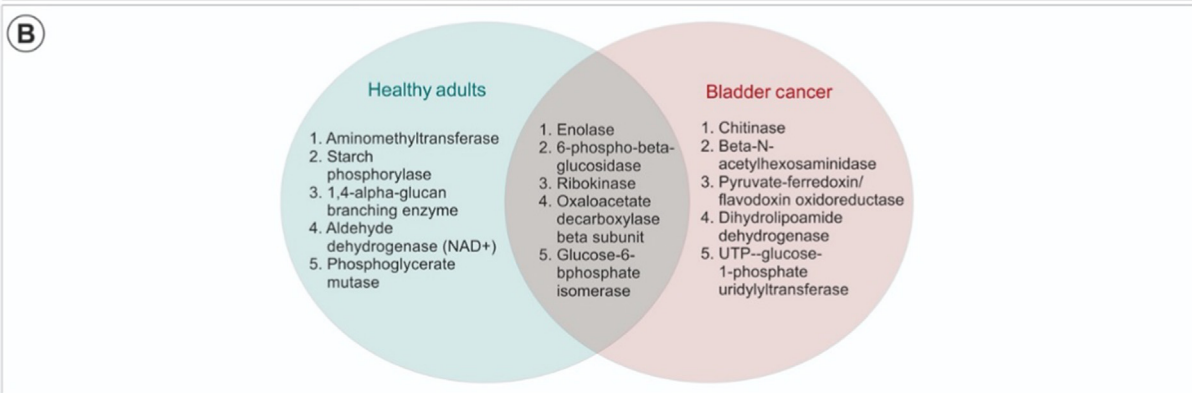
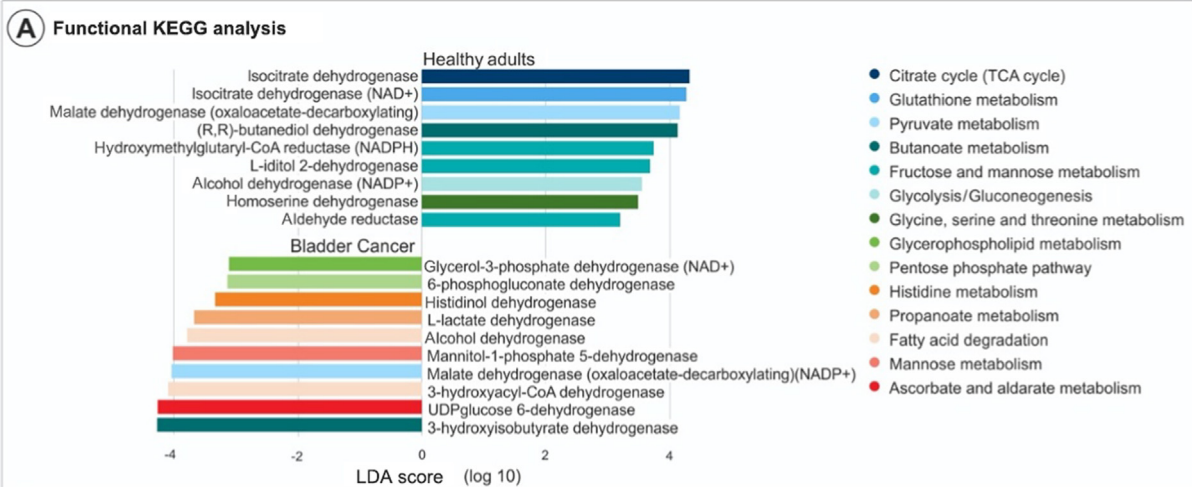


**Fig. 1 – Alterations of enteric fungi in bladder cancer (BCa).** (A) Relative abundance of dominant enteric mycobiome control ( $n = 29$ ) and BCa ( $n = 32$ ) (B) Principal component analysis of Bray-Curtis distance showing stratification of BCa from control samples by fungal composition profile. Distinct clustering between BCa and control groups is noted ( $p = 0.002$ ). Groups were compared using Mann-Whitney  $U$  test. (C) Shannon index diversity indices between BCa ( $n = 29$ ) and control ( $n = 32$ ) groups. (D) Relative fold change in mycobiome species in bladder cancer patients ( $n = 29$ ) against a mean normalized relative abundance of control group ( $n = 32$ ). The greatest difference between *Tremellales* (log change  $-2.99$ ,  $p = 0.0041/p_{adj} = 0.009$ ), *Hypocreales* (log change  $-3.871$ ,  $p \leq 0.001/p_{adj} = 0.003$ ), and *Dothideales* (log change  $-2.37$ ,  $p = 0.002/p_{adj} = 0.016$ ; Fig. 1D) were seen.



second most abundant order, constituting 14.71% of BCa samples. These two orders represented the majority of all fungal compositions across bladder samples, with the most common remainder organisms identified as *Tremellales* (10.96%), *Sporidiobolales* (7.68%), and *Dothideales* (6.18%; Fig. 1A). *Eurotiales* was the third most abundant order, constituting 1.94% of healthy control samples. *Gugnardia*, *Sebacina*, and *Stylonectria* were uniquely found in the healthy cohort and not in the BCa cohort.

The Simpson diversity index of the mycobiome showed significant differences between healthy individuals and BCa patients (0.13 vs 0.29, Wilcoxon rank sum  $p = 0.0038$ ). Similarly, the Shannon diversity index showed a significant difference between the two groups (0.12 vs 0.48, Wilcoxon rank sum  $p = 0.0032$ ). Two-dimensional space using nonmetric multidimensional scaling ordination based on the Bray-Curtis similarity score revealed clustering in the fungal mycobiota composition of healthy controls and BCa patients (Mann-Whitney  $U$  test,  $p = 0.002$ ; Fig. 1B and 1C). Additionally, LEfSe was used to measure fungal composition differences between healthy controls and BCa patients, with the greatest difference between *Tremellales* (log change  $-2.99$ ,  $p = 0.0041/p_{adj} = 0.009$ ), *Hypocreales* (log change  $-3.871$ ,  $p \leq 0.001/p_{adj} = 0.003$ ), and *Dothideales* (log change  $-2.37$ ,  $p = 0.002/p_{adj} = 0.016$ ; Fig. 1D).

### 3.2. Fungal diversity and composition in males and females

We next analyzed the fecal mycobiome difference between males and females. Relative abundance data showed the dominance of *Saccharomycetales* in both males (21.8%) and females (34.6%). *Sebacinales* was the second most abundant order, accounting for 19.5% and 28.9% of male and female samples, respectively. There were no differences in the microbial diversity between male and female samples (Shannon diversity  $p = 0.27$ , Wilcoxon rank sum). Furthermore, there were no difference in organism clustering, as determined by PCoA ordination of unweighted UniFrac distances ( $p = 0.273$ ; Supplementary Fig. 1A–D). An LDA score of  $\geq 3$  was used as a cutoff to support high-dimensional class comparisons, and to evaluate differences between males and females, by coupling standard statistical tests with additional biological encoding and effect relevance. Male BCa samples exhibited higher LDA score *Tremellales* (log change 5.119,  $p < 0.001$ ,  $p_{adj} < 0.001$ ) and lower LDA score *Saccharomycetales* (log change  $-4.686$ ,  $p < 0.001/p_{adj} < 0.001$ ), than those for females BCa samples.

### 3.3. Metabolic characterization and functional biomarkers

To understand the metabolic potential of mycobiome differences in BCa, metagenomes were predicted by PICRUSt

using ITS1/2 rRNA gene amplicon data. Metabolic reconstruction was performed in HUMAnN2, which detected 90 KEGG modules across all BCa samples (Supplementary material). In order to identify preferential genetic investments among the resident fungi of each cohort, we analyzed over-represented KEGG orthology and KEGG modules. A comparison of the function distributions of the metagenome revealed the differential expression of the inferred functions at the genomic and transcriptomic levels, as indicated in Figure 2A. An increased expression ratio of chitinase, beta-N-acetylhexosaminidase, pyruvate-ferredoxin, dihydrolipoamide dehydrogenase, and UTP-glucose-1-phosphate uridylyltransferase was unique to the BCa cohort.

Most of the core modules identified are essential for sustenance of life in the environment (eg, carbohydrate and amino acid metabolism). Among these, 19 modules were differentially expressed between healthy and BCa cohorts (Fig. 2A).

### 3.4. Ecological interactions between differently abundant bacterial and fungal families

To understand the potential interaction between differentially abundant bacteria and fungi of the BCa and control groups, we performed an additional bacterial differential abundance analysis and estimated the ecological network at the taxonomic level (Fig. 2). In the control group, negative interactions were observed between fungal *Boletales* and bacterial *Leptospirales*. In the BCa group, negative interactions were observed between fungal *Chaetomiaceae* and bacterial *Burkholderiales*. Notably, a network analysis for the BCa group revealed a strong negative correlation between fungal and bacterial orders (Supplementary Fig. 2) suggesting dysbiosis in BCa, which may enhance or suppress colonization of certain fungal families.

### 3.5. Mycobiome interaction and chemotherapy response in BCa

We next asked whether mycobiome composition and abundances within the gut were associated with a specific treatment outcome to chemotherapy response (gemcitabine-cisplatin). We sought to determine whether differences exist in the gut mycobiome of patients with CR and NR to therapy. To test this, we first compared the OTUs of CR versus NR, demonstrating an increased prevalence of *Hypocreales* (27.12% vs 0.12%) and lower *Saccharomycetales* (50.34% vs 78.30%) in the CR group (Fig. 3A). Loss of mycobiome diversity (dysbiosis) was seen in the NR group (median alpha diversity 0.26 vs 0.83,  $p = 0.34$ ); although not statistically significant, a clear community separation was noted

Fig. 2 – (A) Differentially abundant KEGG metabolic pathways inferred by LEfSe using KEGG module abundance to identify differentially abundant pathways between controls and bladder cancer patients. PICRUSt was used to predict the functional potential of mycobiome using ITS RNA gene sequence data. The prevalence of top 19 mycobiome-associated KEGG pathways seen in control and healthy gut is presented. (B) Venn diagram analysis showing specific and shared expressed pathways between control and bladder cancer mycobiome KEGG metabolic pathways. Unique KEGG metabolic pathways are identified in the pink (BCa) and blue (controls) regions ( $p < 0.05$ ). (C) Microbiome and mycobiome interaction network built from OTUs; each node represented a microbe or fungus, and each line presents co-occurrence or interaction (green = negative and red = positive). ITS = internal transcribed spacer; KEGG = Kyoto Encyclopedia of Genes and Genomes; LDA = linear discriminant analysis; LEfSe = LDA effect size; PICRUSt = Phylogenetic Investigation of Communities by Reconstruction of Unobserved States; TCA = tricarboxylic acid.

FUNGAL DYSBIOSIS DETERMINES CHEMOTHERAPY RESPONSE IN BLADDER CANCER

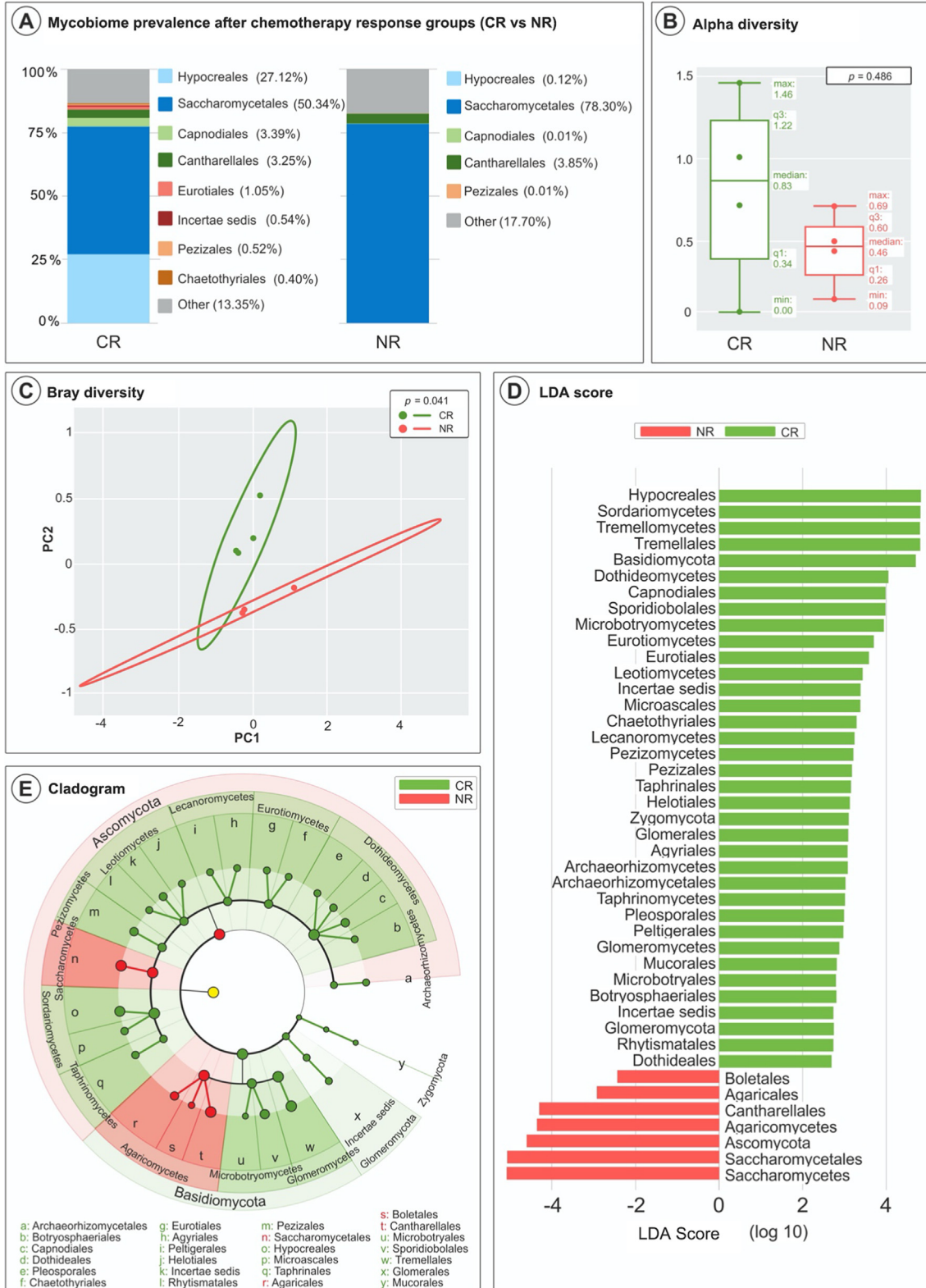


(Fig. 3B). Importantly, upon visualizing beta diversity by PCoA, we found notable clustering effect by response status in the gut mycobiome of these patients ( $p = 0.041$ ; Fig. 3C).

To further explore these significant findings, we then performed high-dimensional class comparisons via LEfSe, which again demonstrated differentially abundant fungi of the CR versus NR group. Particularly, within the NR group, the presence of *Agaricomycetes* and *Saccharomycetes* was significantly enriched (Fig. 3D and 3E).

#### 4. Discussion

In this study, we analyzed the composition and diversity of the fungal mycobiota in patients with BCa compared with healthy controls. Notably, this study is the first to describe and analyze fungal components in BCa. Our study characterizes the intestinal mycobiome and identifies distinct differences between BCa and control patients in alpha diversity and clustering of fungal families. Furthermore, through the LEfSe differential expression analysis, we highlight differences in the prevalence of *Saccharomycetales*, *Tremellales*, *Hypocreales*, and *Dothideales*. While distinct community richness (alpha diversity) and level of similarity and dissimilarity were significantly different between control individuals and BCa patients, we found no differences between genders. Our study further identified BCa-specific shifts in fungal composition, as reflected in the significant enrichment of three orders (*Hypocreales*, *Tremellales*, and *Dothideales*). As <10% of the 1.5 million fungi in the world have been investigated taxonomically, the pathogenic or cytotoxic potentials of these species have not been reported widely in the literature [11]. For instance, the fungal order *Hypocreales* has only recently been shown to produce cytotoxic xanthone-antraquinone heterodimers, with 20S proteasome inhibitory activity [12]. Even more so, fungi have been a valuable source for drug leads (eg, the anticancer drug paclitaxel is produced by endophytic fungi). The interaction between the gut mycobiota and host immunity is complex and contributes to the regulation of local and systemic inflammatory responses, oncogenic signaling, and tumor progression. As such, manipulation of the intestinal microbiota is quickly becoming a consideration in cancer immunotherapy.

In this study, the fungal order *Saccharomycetes* was depleted in BCa patients. This fungal order is a major component of the human gut microbiota, which had been shown to reduce adherent invasive *Escherichia coli* and exhibit regulatory and anti-inflammatory effects on the host by inducing interleukin-10 production [13]. These findings are

consistent with the findings from the colorectal cancer literature, which reports a decrease in commensal *Saccharomycetes* in colon cancer patients [14].

The increased expression ratio of chitinase was unique to the BCa cohort. This secreted glycoprotein has been associated with adverse clinicopathological features in urothelial cancer, including nodal metastasis, high mitotic activity, and shorter disease-free survival (reference). Furthermore, chitinase-like proteins negatively regulate both type 1 T helper and cytotoxic T lymphocyte functions, and decrease tumor suppressor genes [9].

Our results indicate that the gut mycobiome may modulate tumor response to preoperative chemotherapy in BCa patients. We propose that the patients with a “favorable” mycobiome composition (eg, high diversity, and low abundance of *Agaricomycetes* and *Saccharomycetes*) may have enhanced systemic immune response to chemotherapy through antigen presentation. Modulation of chemotherapeutic agents through metabolism, enzymatic degradation, and immunomodulation may in fact alter drug efficacy and anticancer effects. Although our study did not measure additional products of fungal translocation, chemotherapy degradation, and immunomodulation present across mycobiome composition, our findings strongly warrant prompt evaluation in cancer patients through clinical trials or exploratory research.

The alterations of gut bacterial metabolites in the setting of illness, antibiotics, and medications may have indirect effects on fungal biodiversity and tumorigenesis. Mycobiome has been implicated in the pathogenesis of not only colon adenomas [15], but also pancreatic adenocarcinoma, where translocation of *Malassezia* spp. promotes tumorigenesis through activation of complement cascade via activation of mannose binding lectin [16]. Similar to previously published research, and as highlighted in our study, researchers have shown a decrease in *Saccharomycetes* in colorectal cancer [14], although the mechanism is yet to be elucidated.

Our study has several limitations. The results of our study, although unique, do not provide survival analysis. Further translational studies with larger sample size, particularly after neoadjuvant chemotherapy, are needed to validate and evaluate the effect of functional pathways with the goal of therapeutic manipulation or drug repurposing (and potentially “personalized” therapeutic targets). Our study also did not collect samples prior to the initiation of chemotherapy, limiting the analysis of dynamic changes that may occur during treatment. The gut microbiota is affected by the environment, including diet, which our study did not take into account. Further-

**Fig. 3 – Compositional difference in the gut mycobiome associated with neoadjuvant chemotherapy response.** (A) Stacked bar plot of phylogenetic composition of common fungal taxa (>0.01% abundance) at the order level in fecal ( $n = 10$ ) samples by ITS rRNA sequencing. (B) Inverse Simpson diversity scores of the gut mycobiome in the complete response (CR;  $n = 4$ ) versus no response (NR;  $n = 3$ ) to gemcitabine-cisplatin neoadjuvant chemotherapy by Mann-Whitney test. The remainder ( $n = 3$ ) experienced partial response to NAC, with residual low-grade cancer within the specimen. Error bars represent the distribution of diversity scores. (C) Principal coordinate analysis of fecal samples ( $n = 7$ ), with CR ( $n = 4$ ), and with NR ( $n = 3$ ), showing clustering of nonresponders and responders based on mycobiome composition ( $p = 0.041$ ). (D) LDA scores computed for differentially abundant taxa in the fecal mycobiome of the CR (green) and NR (red) groups. Length indicates the effect size associated with designated taxon ( $p = 0.05$  for the Kruskal-Wallis test; LDA score >3). (E) Cladogram of LEfSe showing differences in fecal taxa across mycobiome in the CR versus NR group. Increased abundance of *Agaricomycetes* and *Saccharomycetes* is present in the NR group. ITS = internal transcribed spacer; LDA = linear discriminant analysis; LEfSe = LDA effect size; NAC = neoadjuvant chemotherapy.

more, there are many potential known and unknown confounding factors that may play a role in the gut mycobiome, which we did not adjust in our analysis. Potential confounders such as over-the-counter medications, environmental exposure, prescription medication, and dietary restrictions may influence a person's mycobiome. Despite these limitations, our study is the first to characterize the enteric mycobiome in patients with BCa and describe complex ecological network alterations, indicating complex bacteria-fungi interactions. Further investigations are warranted to identify the functional consequences of the altered mycobiome and to clarify the role of fungi in BCa pathogenesis and treatment.

## 5. Conclusions

Our study is the first to characterize the enteric mycobiome in patients with BCa and describe complex ecological network alterations, indicating complex bacteria-fungi interactions, particularly highlighted among patients with complete neoadjuvant chemotherapy response.

**Author contributions:** Laura Bukavina had full access to all the data in the study and takes responsibility for the integrity of the data and the accuracy of the data analysis.

*Study concept and design:* Bukavina, Mishra, Calaway.

*Acquisition of data:* Bukavina, Sindhani, Abbosh.

*Analysis and interpretation of data:* Sindhani, Bukavina, Ginwala, Sarah Markt.

*Drafting of the manuscript:* Bukavina, Prunty.

*Critical revision of the manuscript for important intellectual content:* All authors.

*Statistical analysis:* Bukavina, Sindhani, Abbosh, Ginwala.

*Obtaining funding:* Uzzo, Ponsky, Ghannoum, Calaway, Sarah Markt.

*Administrative, technical, or material support:* Uzzo, Ponsky, Ghannoum, Calaway, Sarah Markt.

*Supervision:* Abbosh.

*Other:* None.

**Financial disclosures:** Laura Bukavina certifies that all conflicts of interest, including specific financial interests and relationships and affiliations relevant to the subject matter or materials discussed in the manuscript (eg, employment/affiliation, grants or funding, consultancies, honoraria, stock ownership or options, expert testimony, royalties, or patents filed, received, or pending), are the following: None.

**Funding/Support and role of the sponsor:** This work was supported by P30CA043703 Case Comprehensive Cancer Center Microbiome Grant and P30 CA006927 Fox Chase Cancer Center Support Grant. Mahmoud Ghannoum has funding from National Institutes of Health (NIH grant # R01AI145289-01A1).

## Appendix A. Supplementary data

Supplementary data to this article can be found online at <https://doi.org/10.1016/j.euro.2022.06.005>.

## References

- [1] Saginala K, Barsouk A, Aluru JS, Rawla P, Padala SA, Barsouk A. Epidemiology of bladder cancer. *Med Sci (Basel)* 2020;8:15.
- [2] Sanli O, Dobruch J, Knowles MA, et al. Bladder cancer. *Nat Rev Dis Primers* 2017;3:17022.
- [3] Gomez A, Luckey D, Taneja V. The gut microbiome in autoimmunity: sex matters. *Clin Immunol* 2015;159:154–62.
- [4] Berg G, Rybakova D, Fischer D, et al. Microbiome definition revisited: old concepts and new challenges. *Microbiome* 2020;8:103.
- [5] Walters W, Hyde ER, Berg-Lyons D, et al. Improved bacterial 16S rRNA gene (V4 and V4–5) and Fungal internal transcribed spacer marker gene primers for microbial community surveys. *mSystems* 2016;1:e00009-e15.
- [6] Caporaso JG, Kuczynski J, Stombaugh J, et al. QIIME allows analysis of high-throughput community sequencing data. *Nat Methods* 2010;7:335–6.
- [7] Navas-Molina JA, Peralta-Sánchez JM, González A. Advancing our understanding of the human microbiome using QIIME [Chapter 19]. In: DeLong EF, editor. *Methods in enzymology*. Academic Press; 2013. p. 371–444.
- [8] Shannon PT, Grimes M, Kutlu B, Bot JJ, Galas DJ. RCytoscape: tools for exploratory network analysis. *BMC Bioinformatics* 2013;14:217.
- [9] Li J, Jia H, Cai X, et al. An integrated catalog of reference genes in the human gut microbiome. *Nat Biotechnol* 2014;32:834–41.
- [10] Langmead B, Salzberg SL. Fast gapped-read alignment with Bowtie 2. *Nat Methods* 2012;9:357–9.
- [11] Hawksworth DL, Rossman AY. Where are all the undescribed fungi? *Phytopathology* 1997;87:888–91.
- [12] Ayers S, Graf TN, Adcock AF, et al. Cytotoxic xanthone-anthraquinone heterodimers from an unidentified fungus of the order Hypocreales (MSX 17022). *J Antibiotics* 2012;65:3–8.
- [13] Jawhara S, Habib K, Maggioletto F, et al. Modulation of intestinal inflammation by yeasts and cell wall extracts: strain dependence and unexpected anti-inflammatory role of glucan fractions. *PLoS One* 2012;7:e40648.
- [14] Coker OO, Nakatsu G, Dai RZ, et al. Enteric fungal microbiota dysbiosis and ecological alterations in colorectal cancer. *Gut* 2019;68:654–62.
- [15] Luan C, Xie L, Yang X, et al. Dysbiosis of fungal microbiota in the intestinal mucosa of patients with colorectal adenomas. *Sci Rep* 2015;5:7980.
- [16] Aykut B, Pushalkar S, Chen R, et al. The fungal mycobiome promotes pancreatic oncogenesis via activation of MBL. *Nature* 2019;574:264–7.